Raising Flags: Applications of Chemical Marker Groups To Study Self-Assembly, Chirality, and Orientation of Interfacial Films by Scanning Tunneling Microscopy

LEANNA C. GIANCARLO AND
GEORGE W. FLYNN*

Department of Chemistry and Columbia Radiation Laboratory, New York, New York 10027

Received August 4, 1999

ABSTRACT

When used in conjunction with "chemical marker groups" (functionalities such as −Br and −COOH), scanning tunneling microscopy is a powerful tool for studying the properties of liquid−solid interfaces. Chemical markers serve as "flags" for the identification of interfacial structures, allowing, for example, the absolute chirality of optically active molecules self-assembling on a graphite surface to be determined. Subtle changes in the orientation of these chemical functionalities that affect the long-range order of interfacial films have also been observed and explored. Finally, alterations in self-assembly resulting from variations in adsorbate or substrate structure can be deduced by taking advantage of these STM "flags".

I. Introduction

Since its invention nearly two decades ago, scanning tunneling microscopy (STM) has become an essential tool for researchers working at the interface between various scientific disciplines including chemistry, physics, material science, and environmental studies. STM's multidisciplinary appeal lies in its ability to image samples under virtually all experimental conditions with *atomic* resolution. From its inception in 1982 by Binnig and Rohrer,[1] STM and other subsequent "optic-less" scanning probe microscopies (SPMs), e.g., atomic,[2−4] chemical,[5] magnetic,[6]

and electrostatic force,[7] have been employed at the forefront of surface and interfacial research to examine those issues essential to future technological advances in such far-reaching areas as nanoscale engineering, biosensor development, catalysis, and electronics.

Initial STM studies probed bare metal and semiconductor surfaces under the most pristine, ultrahigh-vacuum conditions.[8−10] With the aid of improved instrumentation and theoretical tools, investigations of molecules adsorbed on these "clean" substrates quickly followed. Recently, STM has been used under ambient conditions and at liquid−solid interfaces (including electrochemical environments) to investigate the structure and dynamics of bare and adsorbate-covered surfaces of "real" systems in situ with molecular, submolecular, and even atomic resolution.

One of the principal focuses of interfacial STM studies under ambient conditions addresses questions of molecular self-assembly. While a plethora of SPM research is currently being conducted on chemisorbed, self-assembled monolayers,[11−16] an equally stimulating and challenging area is the investigation of self-assembled systems *physisorbed* at the liquid−solid interface. The issues at the heart of these studies are (1) the nature of the forces governing molecular organization on the surface, (2) the roles of adsorbate−adsorbate versus adsorbate−substrate interactions in driving and stabilizing molecular order, (3) the relationship between two-dimensional structure observable by STM and three-dimensional crystalline ordering, and (4) the design and control of interfacial assemblies. In many cases, the two-dimensional molecular self-ordering examined via STM is representative of the bulk crystalline structure for the molecule;[17] however, due to the presence of and interactions with the surface, some molecular assemblies are formed with properties not found in their three-dimensional crystal structure.[18−22] In these cases, the surface acts as a template upon which new patterns of organization are formed. One such example, involving creation of two-dimensional chiral assemblies at the liquid−solid interface from a three-dimensional racemic mixture, is described below.

In this Account we describe the identifigation and use of STM "chemical marker groups" to interpret patterns of molecular ordering and conformations of individual molecules. "Marker groups" are chemical functional groups that exhibit unusual contrast in the STM images relative to the rest of the atoms in a molecule; the thiol end group (−SH) provides a vivid example of such a marker. Thiols (such as $CH_3(CH_2)_nSH$, $n = 17, 21$) lie flat and assemble into ordered arrays on the basal plane of graphite; however, regions of topographic protrusions, indicative of increased electron tunneling probability, appear scattered throughout the STM images.[23−26] These regions are readily attributed to the location of the sulfur atom in the thiol functionality, and their presence provides a measure of the level of disorder for these self-assembled films. Even

more powerful is the combination of two chemical markers within the same molecule, such as a bromine atom and a carboxylic acid group, which provide remarkable information about two-dimensional self-assembly at the liquid−solid interface. The unusual contrast of these marker groups can be attributed to a combination of factors related to the electronic structure, size, and spatial orientation of the chemical functionality. Here, we show specific examples of how STM can be used in conjunction with these "double marker groups" to (1) determine molecular conformations and assign *absolute* chirality, (2) deduce subtle differences in patterns of monolayer ordering between nearly identical molecules, and (3) elucidate changes in self-assembly due either to orientational variations within the adsorbate or to the physical and electronic properties of specific substrates.

II. "Single Chemical Markers" in STM

Although STM images, which are essentially plots of electron tunneling probability versus surface position, provide atomic-level resolution of surface features, there is currently no general method for deducing the chemical identity of an atom in an STM image. Rather, direct identification of individual atoms or molecules is relatively unusual, requiring the use of some form of "marker" that stands out in the STM image.[14,15,27−35] Even as heavy atoms have been used to elucidate three-dimensional crystal structure by X-ray crystallography, "chemical marker groups" can be used to assist in the identification of both specific atoms within a two-dimensional assembly and the pattern of self-organization. Three types of STM chemical markers have been reported thus far: those that have enhanced tunneling probability and appear as topographic protrusions relative to the remainder of the molecule, those that have decreased tunneling probability and appear as depressions, and those that can undergo an inversion in contrast, alternating between protrusions and depressions.

Among the substituents on long-chain molecules that exhibit enhanced tunneling probability (topographic protrusions) in STM images are $-SH$, $-S-$, $-SS-$, $-I$, $-NH_2$, $-O=CNH_2$, $C=C$, $C\equiv C$, and aromatic rings.[24,25,36−39] An interesting correlation between these groups and their relative image contrast (tunneling probability) can be made on the basis of their range of ionization potentials. The ionization potential (IP) for these functionalities provides a qualitative measure of the extent of electronic coupling between the adsorbate and the graphite surface.[36] A lower ionization potential (i.e., a value closer to the work function of the surface) corresponds to more favorable coupling between the orbitals of the molecule and those of the substrate and, thus, stronger interaction between the adsorbate electronic levels and the surface Fermi level.[36,40,41] Chemical markers that appear as protrusions have IPs in the range of 7−9 eV (for C_4H_9X), values

that lie between the work function of graphite (5.7 eV) and the ionization potential for an unsubstituted hydrocarbon (10.5 eV for C_4H_{10}).[42]

The presence of topographic depressions, areas of decreased tunneling probability, has also been noted in STM investigations of functionalized long-chain molecules. Specifically, $-F$, $-COOH$, $-C\equiv N$, and to a lesser degree $-OH$ exhibit lowered tunneling probability compared to the rest of the molecular chain.[36,43−45] The correspondence between ionization potential and STM image contrast also predicts that groups with larger ionization potentials (IP $\geq$ 11 eV),[42] marker groups showing topographic depressions, are more poorly coupled to a surface such as graphite, resulting in reduced electron tunneling in the vicinity of such substituents. An example of a chemical marker exhibiting a topographic depression is shown in Figure 1a for the self-assembly from a phenyloctane solution of octadecanoic acid ($CH_3(CH_2)_{16}$-COOH) on graphite. On either side of one molecular length, highlighted with a black bar, dark circular regions are found that correspond to topographic depressions. These regions are attributed to the locations of the hydrogen-bonding carboxylic acid groups of adjacent molecules. The "circular" shapes arise from the interdigitating pattern of molecules schematically represented to the right of the STM topograph. When most unsubstituted carboxylic acids order at the interfacial region, two carboxylic acid groups of neighboring molecules hydrogen bond together.[37,39,43,44,46] The next pair of molecules within the same row then organize with the methyl ends next to each other, and the pattern repeats.

Finally, at least one STM chemical marker, bromine atoms, can sometimes alternate between a topographic protrusion and a depression.[24,25] As displayed in Figure 1b, 1-bromodocosane ($CH_3(CH_2)_{21}Br$) forms ordered, two-dimensional arrays at the phenyloctane−graphite interface. A single molecule is marked by the black bar. Note that on either side of this bar dark troughs, labeled 1 and 2, are present. After several minutes, the STM topograph of Figure 1b undergoes a dramatic transformation into the image depicted in Figure 1c. Now, every other trough (see the trough marked as 2) appears with "bright" contrast. These bright regions (areas of topographic protrusion) are ascribed to the locations of the terminal bromine atoms. The variation in contrast between the images in Figure 1b and c results from an energetically allowed rotation of the Br end group from a configuration where the chemical marker lies within the plane of adsorbed molecules (see molecular model to the right of Figure 1b) to one where the Br atom points up, closer to the STM tip (see molecular model to the right of Figure 1c).[24,25] In the latter case, as confirmed by recent theoretical calculations,[47] a favorable overlap exists between the brominated molecular end and the STM probe since the electron density of the adsorbate−substrate complex has been pushed up nearer to the tip. Here, the geometry of the end group becomes the dominant factor providing an STM marker. Although a functional group with alternating contrast poses some difficulty in labeling surface-adsorbed mol-
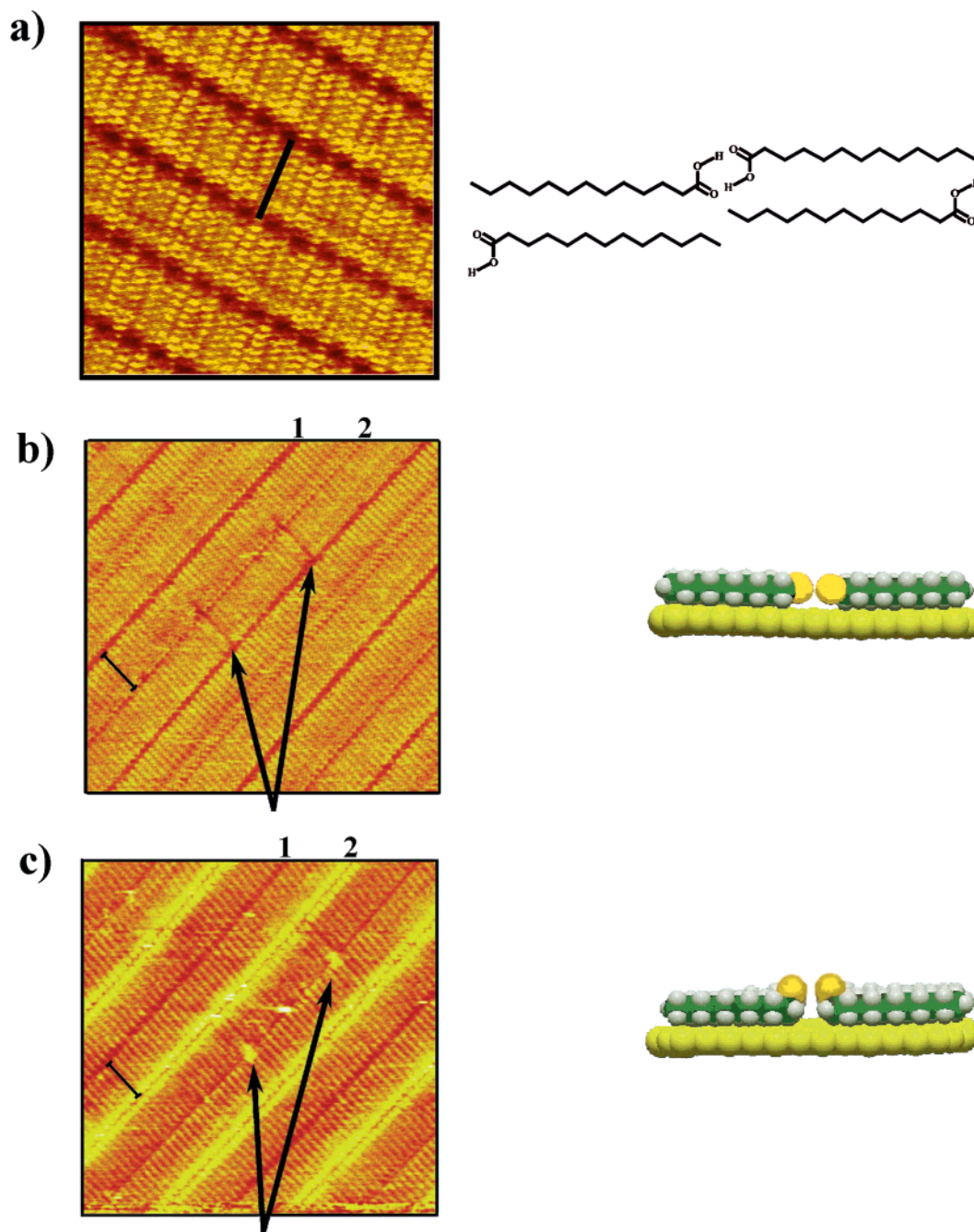
FIGURE 1. (a) 9 × 9 nm^2 constant current image of octadecanoic acid self-assembled on graphite (1.4 V bias (sample negative), 300 pA current). The dark circular regions at the molecular ends (black bar denotes one molecule) are assigned as the location of the hydrogen-bonding COOH groups. At right, a schematic representation of the interdigitating pattern formed by the self-assembly of octadecanoic acid shows the alternating COOH and CH$_3$ groups in the direction perpendicular to the molecular axis. (b) 20 × 20 nm^2 STM topograph of 1-bromodocosane imaged at the phenyloctane−graphite interface. One molecular length (black bar) is bordered by wide and narrow troughs, labeled 1 and 2, respectively. The arrows point to defects in the two-dimensional adlayer. To the right of the image, a side-view molecular model depicts the orientation of the terminal Br atoms (yellow balls) relative to the hydrocarbon backbone, resulting in the "dark" (topographically depressed) conformation. (c) Same area of the physisorbed assembly as in (b) approximately 10 min later. Note the location of the defects. Now, the areas labeled 2 appear "bright" and are attributed to the location of the Br end groups. The molecular model at the right shows that the terminal Br atoms are raised relative to the rest of the thin film, increasing the interaction between the Br chemical marker and the tip. Scan parameters for both (b) and (c) are 1.5 V (sample negative) and 400 pA in constant current mode.

ecules, such fluctional markers can serve as powerful diagnostics for dynamic processes taking place at interfaces. This is particularly true when studies can be carried out over a range of temperatures, as has been shown in NMR investigations of fluctional protons.[48]

III. Application of "Double Chemical Marker Groups" in STM

Determination of Molecular Conformation: Assignment of Absolute Chirality. The carboxylic acid and Br atom
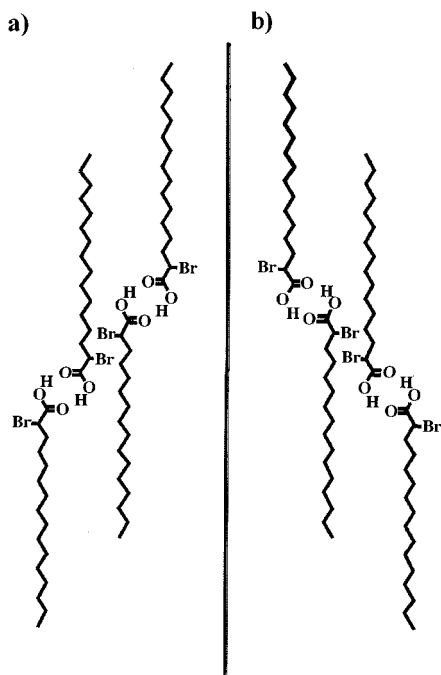
a)   b)

FIGURE 2. Schematic representation of (*R*)/(*S*)-2-bromohexade-canoic acid. The left-hand side depicts the *R* conformer, while the right-hand side shows the *S* enantiomer. The black vertical line is a reflection plane emphasizing that these two conformers are mirror images of one another. As with other carboxylic acids, 2-bromo-hexadecanoic acid hydrogen bonds through the carboxyl group to give an alternating pattern of Br—COOH—Br. In (a) this pattern runs from lower left to upper right (*R* conformer) and in (b) from upper left to lower right (*S* isomer).

chemical marker groups of Figure 1a and c can be used within the same molecule, on the same carbon atom, in fact, to determine the *absolute* molecular conformation of individual molecules. Specifically, these groups have been used to assign the chirality for molecules of (*R*)/(*S*)-2-bromohexadecanoic acid physisorbed on a graphite substrate.[49] Both enantiomers are represented schematically in Figure 2. Attached to each chiral carbon is the topographically depressed carboxylic acid group, a bright "protruding" bromine atom (on the carbon alpha to the COOH group), the alkyl chain, and a hydrogen atom (not explicitly shown). To maximize energetically favorable interactions when self-assembling at the liquid—solid interface, the acid end groups hydrogen bond to each other. This relatively strong "nonbonded interaction" plus a weaker attraction between the bromine atoms on neighboring molecules result in an alternating pattern within the two-dimensional film that has Br—COOH—Br running at a 45° angle to the molecular axis. Figure 2a depicts the *R* isomer, where this pattern runs from lower left to upper right. Its mirror image, the *S* enantiomer, is reflected through the plane indicated by the vertical bar shown in Figure 2b. Here, the Br—COOH—Br pattern proceeds from lower right to upper left.

When a racemic mixture of 2-bromohexadecanoic acid self-assembles from a solution of phenyloctane on the basal plane of graphite, domains are formed as shown in Figure 3. The chiral nature of each domain can be seen by considering the pattern described in Figure 2. In Figure

3a, the alternating pattern of dark and bright spots (acid and bromine atom markers) is clearly visible, running from the lower left-hand corner of this constant current topograph to the upper right, as marked by the direction of the arrow (following the pattern depicted in Figure 2a). The domain pictured in Figure 3b reveals this pattern as starting at the lower right-hand corner and extending to the upper left (as in Figure 2b), the exact mirror image of the domain pictured in Figure 3a!

More careful inspection of these domains permits the absolute chirality of individual 2-bromohexadecanoic acid molecules to be assigned. Figure 4 contains a magnified view of a portion of the image shown in Figure 3a. Again, the topograph is dominated by the pattern of dark depressions and bright protrusions. The topographic depressions are attributed to the locations of the hydrogen-bonding carboxylic acid groups (designated COOH in Figure 4), and the protrusions are ascribed to the positions of the bromine atoms (labeled Br), raised above the plane of the molecular film toward the tip. These protruding Br atoms, adjacent to the "topographically depressed" acid end groups, define the orientation of the rest of the molecule in the self-assembly. For instance, when the "bright" bromine atom lies above the central, "dark" spot, the rest of the alkyl chain does as well. One hydrogen atom for each methylene carbon of this alkyl chain, numbered 1—14, is visible in this high-resolution image.

Knowledge of the positions of these —BR, —COOH, and alkyl chain groups on the chiral carbon allows the absolute conformation of the molecules within this array to be determined. The molecules imaged in Figure 4 are thereby uniquely assigned as *R* enantiomers of 2-bromohexade-canoic acid on the basis of the placement of the marker groups. The two domains depicted in Figure 3a and b, therefore, contain exclusively *R* and *S* isomers, respectively.

The three-dimensional crystal structure of 2-bromo-hexadecanoic acid is comprised of *R* and *S* enantiomers bonded together through the carboxylic acid group.[50] On the two-dimensional graphite surface, however, there is no evidence for an assembly whose unit cell is an *R*—*S* (or *S*—*R*) bonded pair. Instead, as demonstrated in Figures 3 and 5a, paired structures of the same chirality are found exclusively. A simple argument suffices to explain the fact that *R*—*S* paired moieties do not form energetically stable structures relative to either the *R*—*R* or *S*—*S* combinations at the two-dimensional interface of graphite and phenyl-octane. A possible *R*—*S* pair of molecules is shown in Figure 5b. Here, the *R* conformer has a Br atom in the up position (pointed toward the tip), the COOH and alkyl groups lying within a plane parallel to the graphite surface, and the hydrogen atom of the chiral carbon directed toward the surface lattice. This configuration is similar to the proposed structures for unsubstituted *n*-carboxylic acids on graphite and is, therefore, expected to be thermodynamically favorable.[37,39,43,44,46] The *S* enantiomer in this pair also has the COOH and alkyl groups lying in a plane parallel to the graphite substrate; however, now the positions of the hydrogen and bromine on the chiral
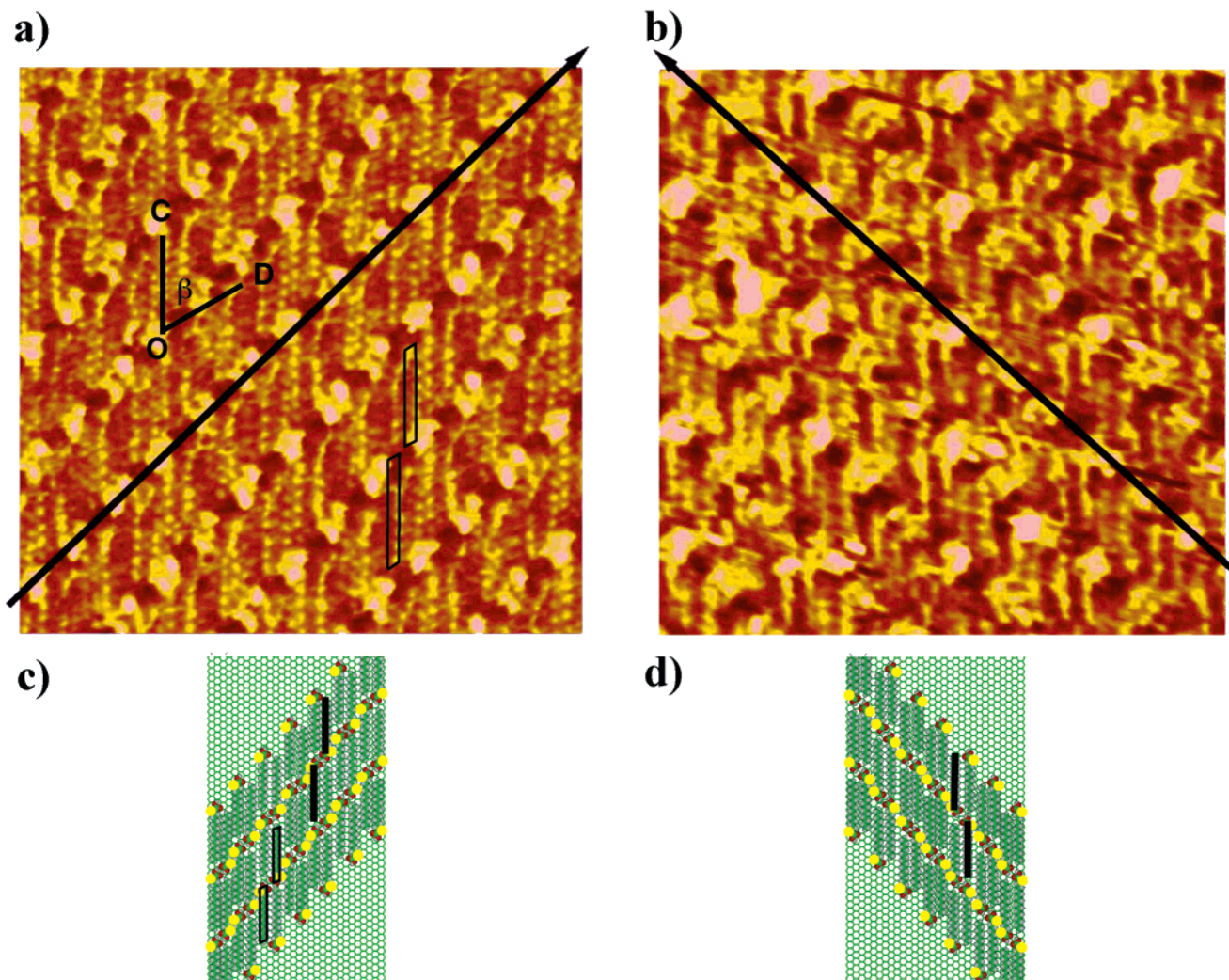
FIGURE 3. (a) STM topograph of one of the domains formed by the assembly of (*R*)/(*S*)-2-bromohexadecanoic acid on graphite. The "bright" topographic protrusions are assigned as the positions of the α Br atoms, while the adjacent "dark" topographic depressions correspond to the hydrogen-bonding COOH groups. An alternating pattern of "bright"—"dark"—"bright" runs through the image from lower left to upper right, as denoted by the black arrow. This domain has been assigned as containing *R* enantiomers exclusively. Two parallelograms denote a hydrogen-bonded molecular pair lying flat on the surface. The angle β formed by the molecular axis, OC, and the direction of the hydrogen bond, OD, has been measured as 53 ± 5°. (b) A second domain of 2-bromohexadecanoic acid molecules found at the phenyloctane-graphite interface. The alternating "bright"—"dark"—"bright" pattern now extends from lower right to upper left in the topographic image. This domain is the mirror image of that shown in (a) and is comprised only of the *S* enantiomer. Both (a) and (b) are 12 × 12 nm² images (1.4 V bias (sample negative), 300 pA tunneling current). (c) A molecular model of (*R*)-2-bromohexadecanoic acid organized on a graphite lattice based on the image shown in (a). The black bars denote a chiral pair of *R*—*R* molecules bonded through their carboxylic acid groups. The yellow circles represent Br, the red balls oxygen, the green areas carbon, and the white spheres hydrogen atoms. The alternating pattern seen in the STM image is also reproduced here. Further, as indicated by the parallelograms, the dimerized acid molecules occupy four rows of the graphite surface. (d) Molecular model representing the STM image of (b). Here, only *S* enantiomers are depicted, and the black bars denote an *S*—*S* chiral pair. Again, the alternating Br—COOH—Br pattern is shown.

carbon are reversed. The hydrogen atom points up toward the tip, while the bromine atom is directed downward into the graphite surface. Due to its relative bulk (C—Br bond distance = 1.937 Å, C—H = 1.101 Å; Br van der Waals radius = 1.95 Å, H = 1.2 Å), Br will push the alkyl portion of the molecule away from the surface, decreasing the van der Waals interaction between the hydrogen atoms of the adsorbate and substrate. This leads to a less stable surface structure that can be easily replaced from solution by a more favorable one consisting of molecules with the same chirality.

A second possibility for an *R*—*S* molecular pair is depicted in Figure 5c. Again, the *R* enantiomer is modeled as described above; however, now the *S* conformer has been constructed by rotating the *S* molecule shown in Figure 5b about the chiral carbon—carboxyl carbon bond. The resulting *R*—*S* pair forms a "herringbone" pattern on the graphite surface, reminiscent of shorter chain length alcohols.[17] For *R*—*R*- and *S*—*S*-based assemblies, part of the stability in the overall two-dimensional array derives from the favorable interactions between the bromine atoms of adjacent molecules lying close to each other and from interactions between the alkyl chain and the substrate (Figure 3c and d). In the "herringbone" *R*—*S*
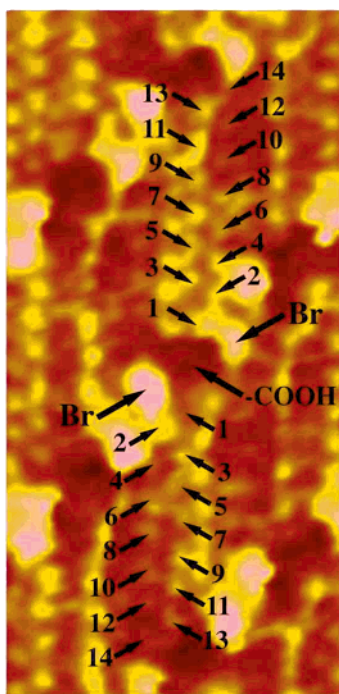
FIGURE 4. High-resolution, magnified portion of the STM image of Figure 3a. The "dark" depressions are assigned as the hydrogen-bonding carboxylic acid groups (marked COOH), and the "bright" protrusions are ascribed to the Br atoms at the α position (labeled Br). The small protrusions, numbered 1–14, correspond to the hydrogen atoms on each methylene carbon of the alkyl chain, pointing up toward the STM tip. Knowledge of the locations of these three groups on the chiral center allows these molecules to be assigned uniquely as *R* enantiomers.

monolayer, the interactions between Br atoms decreases; the Br of one (e.g., *R*) molecule lies next to the hydrogen atom of the adjacent (*R*) molecule. Further, as shown in Figure 5c, the alkyl tail of the *S* enantiomer comes out of registry with the graphite lattice, leading to a less stable adsorbate structure. For these reasons, we believe, this "herringbone" pattern has not been observed by STM for 2-bromohexadecanoic acid molecules physisorbed on graphite. Further, the images of Figure 3 reveal that the graphite acts as a template to separate energetically the isomers of the racemic (*R*)/(*S*)-2-bromohexadecanoic acid mixture despite the fact that the surface itself is *achiral*. The combination of adsorbate–adsorbate *and* adsorbate–substrate interactions forces the self-assembling molecules to segregate on the surface, driving the array to order into chiral domains.

Deducing Subtle Differences in Patterns of Monolayer Ordering: The Impact of One CH₂ Group. Subtle changes in molecular structure can have a significant effect on the packing arrangement of weakly bound adsorbates.[22,51] For alkanes and alcohols (as well as unsubstituted carboxylic acids), the pattern of the molecular array is determined by long-range ordering interactions; therefore, a small change in the length of these molecules has little, if any, effect on the pattern of molecular organization at the surface.[23–25,52,53] When these types of molecules have substituents at opposite ends, however, a change of a

single methylene group along the chain can dramatically influence self-assembly.

Consider the two molecules shown schematically in Figure 6, 12-bromododecanoic ($Br(CH_2)_{11}COOH$) and 11-bromoundecanoic acid ($Br(CH_2)_{10}COOH$), both of which contain two different chemical marker groups, −Br and −COOH.[51] When 12-bromododecanoic acid physisorbs onto graphite from a phenyloctane solution, the STM image reveals areas of "bright" and "dark" spots covering the surface, as can be seen in Figure 7a. On the basis of comparison to work on singly substituted brominated hydrocarbons[24,25] and unsubstituted carboxylic acids,[37,39,43,44,46] the "bright" protrusions are ascribed to the positions of the Br end atoms, while the "dark" depressions are attributed to the hydrogen-bonding carboxyl groups at the other end of the molecule. The presence of these two marker groups allows us to identify individual molecules, demarcated by the black bar OA in the topograph, from within the self-assembled monolayer. Further, each of the smaller spots located between the bromine atom and the COOH group, numbered 1−11 in the image, is assigned to the position of one hydrogen atom on each methylene carbon of the acid backbone protruding up toward the STM tip.

From the assignment of one molecular length, the Br atoms on adjacent molecules are seen to lie next to each other (head-to-head configuration), forming a "dimer" pair. For 12-bromododecanoic acid these pairs have periodic structures of three pairs (containing the black bar), two pairs (above the bar), or one pair. This patterning also illustrates that long-range order persists in the direction parallel to the long hydrocarbon axis, while only local order is present in the direction normal to it.

When 11-bromoundecanoic acid is viewed at the liquid−solid interface by STM, a similar, albeit less well-resolved, image is also obtained (Figure 7b).[51] Again, the "bright" topographic protrusions are assigned as the locations of the −Br functionalities, and the carboxylic acid end groups appear as "dark" topographic depressions. One molecular length is marked by the black bar in the figure. As with 12-bromododecanoic acid, the 11-carbon-long moiety also orders into "dimer" pairs, where now periodic structures containing one or three pairs dominate on the graphite surface.

Detailed analysis of these STM images unveils even more interesting structural changes in the self-assemblies resulting from the loss of a single methylene group. A representation of the monolayer organization for 12-bromododecanoic acid has been constructed in Figure 7c on a graphite template based on the topograph shown in Figure 7a. From this molecular model, it is evident that these brominated, even-chain-length acids adopt a staggered up−down configuration on the substrate. In the complementary model of the 11-bromoundecanoic acid assembly, Figure 7d, however, the odd-length carboxylic acid molecules orient in an upward stairlike progression. These dissimilar structures are a direct result of the change in molecular length of one carbon unit. As depicted in Figure 6a, the −Br and −COOH (particularly, −OH)
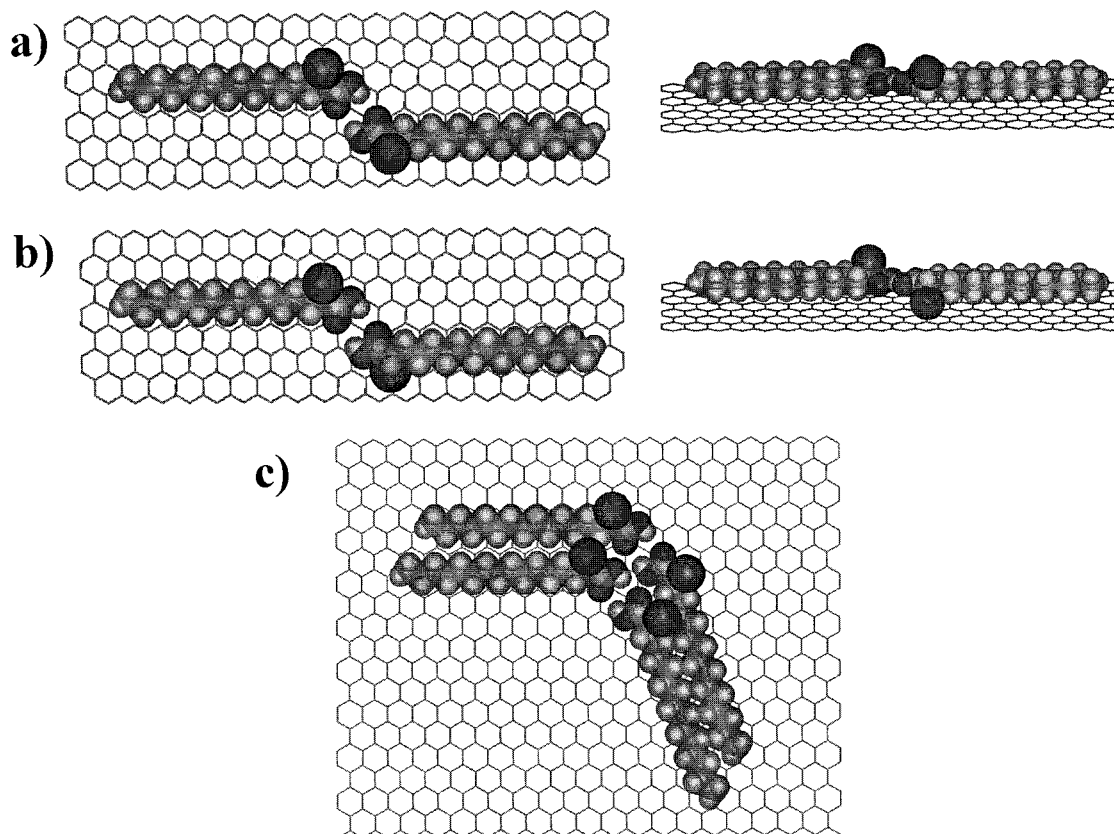
FIGURE 5. (a) Schematic representation of a chiral, *R–R*, pair of 2-bromohexadecanoic acid molecules on a graphite template. The left portion displays a top view of the hydrogen-bonded molecules. The large dark circle represents the Br atom at the α position. Note the favorable registry between the alkyl tail of the molecules and the graphite lattice. At right, a side view is shown where both Br atoms clearly point upward to interact favorably with the STM tip. (b) A schematic depiction of an *R–S* assembly of 2-bromohexadecanoic acid molecules on graphite. The left molecule of the pair is the *R* conformer, and the right is the *S*. The Br atom is shaded black. In the side view model (right), the Br of the *S* enantiomer points down into the sheet of graphite, raising the alkyl tail away from the surface, leading to an unstable adsorbate–surface structure. (c) A second possible model for an *R–S* pair of molecules on graphite. The left molecules are *R* conformers, while the *S* isomers have been rotated 180° about the carboxyl carbon–α carbon bond. Now, both Br atoms of the *S* molecules are directed up near the tip, but the *R* and *S* racemates form a "herringbone" pattern on the surface. This structure has not been observed in the STM images (Figure 3) and is expected to be energetically unstable, as discussed in the text.

chemical marker groups for 12-bromododecanoic acid lie on the same side of the molecular axis. This orientational effect dictates the relationship among the molecules in the assembled monolayer. For a molecule to hydrogen bond to the COOH group of the center bromododecanoic molecule in Figure 6a, this second molecule must shift upward from the central one. Likewise, to maximize interactions between the Br end atoms, a molecule coming from the left must also move up relative to the central brominated acid. This displacement of molecules to optimize adsorbate–adsorbate interactions yields the up–down–up profile seen in the STM image of Figure 7a and the model in Figure 7c. In the case of 11-bromoundecanoic acid, the −Br and −COOH (−OH) groups are positioned on opposite sides of the long molecular axis, as indicated in Figure 6b. Now, maximization of the Br–Br interaction requires the molecule on the left to shift down relative to the central molecule. This results in an upward stairlike progression. The −Br and −COOH marker groups, therefore, have provided "flags" to distinguish the effects of a seemingly minor change in the relative end

group orientation of nearly identical molecules self-assembled at the phenyloctane–graphite interface.

Elucidating Adsorbate and Substrate Induced Variations in Conformation and Self-Assembly. These same markers can also be used to gain insight into how identical chemical groups, arranged in different orientations, affect monolayer ordering. This orientational control of long-range ordering can have important implications for the chemical and physical properties of films formed via self-assembly. We consider two of the molecules described above, 12-bromododecanoic acid and (*R*)/(*S*)-2-bromo-hexadecanoic acid, and explore how the substituents next to the carboxylic acid group can change the relative conformation of this group.[54]

For unsubstituted *n*-carboxylic acids in the gas phase, only a small energy barrier of 1.47 kcal/mol exists for rotation about the carboxyl carbon-to-α-carbon bond. (Even for carboxylic acids brominated at the α position, this barrier is only 2.34 kcal/mol.[55]) The two all-trans orientational variations of the carboxyl group with respect to the alkyl chain are depicted schematically in Figure 8. When these same molecules physisorb onto graphite at
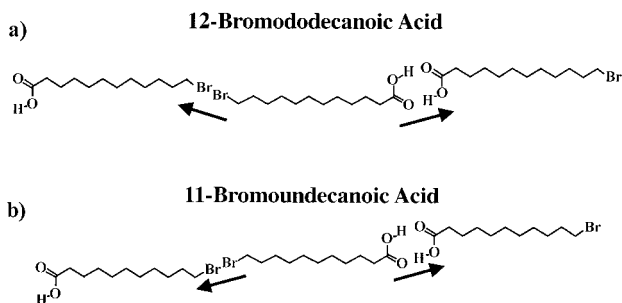
a)

12-Bromododecanoic Acid

b)

11-Bromoundecanoic Acid

FIGURE 6. (a) Schematic representation of a 12-bromododecanoic acid assembly. The carbon-to-Br and carbon-to-carboxyl hydrogen bonds point in the same direction (up) relative to the long, molecular axis. For molecules to assemble around the central one, each substituted fatty acid must shift upward to maintain favorable adsorbate—adsorbate interactions (hydrogen-bonding at one end and Br—Br van der Waals-like attractions at the other end). An "up"—"down"—"up" progression on the surface results. (b) Schematic representation of an assembly of 11-bromoundecanoic acid molecules. In this case, the carbon—Br bond and carboxylic acid—hydrogen bond point in opposite directions relative to the hydrocarbon backbone. For molecules to assemble around the center acid, the left molecule must shift downward, while the right shifts upward, yielding an upward "stairlike" profile.

the liquid—solid interface, the nearly free rotation of the acid end group is hindered, "freezing" the orientation of the carboxyl group. As shown in Figure 8a and b, respectively, the angle describing the relative orientation of the hydroxyl group to the long molecular axis can have one of two values: $\alpha = 25°$ or $\beta = 46°$. In addition, the area that a hydrogen-bonded "dimer" of acid molecules occupies on the graphite surface depends on this angle. For acids in which the angle is $\alpha = 25°$, a dimer pair of molecules takes up three rows of the graphite substrate; when the angle is increased to $\beta = 46°$, four rows become covered by the hydrogen-bonded pair.

As noted above, when 12-bromododecanoic acid physisorbs onto a graphite surface, the molecules hydrogen bond together through their carboxyl groups, represented by the dark areas in the STM topograph of Figure 7a.[51] The Br atom at the opposite end of the molecule appears as a "bright" topographic protrusion. The molecular axis (OA) is defined by the small spots, which are assigned as hydrogens along the backbone of the molecule (encased by the parallelogram in Figure 7a), between these two marker groups. The direction of the hydroxyl group (OB) can be determined by the short edge of the dark areas (attributed to the COOH groups). This yields a molecular axis-to-hydroxyl angle (BOA), α, of $25 \pm 1°$, as marked in the figure. Molecular models of a portion of 12-bromododecanoic acid assembled on a graphite template, shown in Figure 7c, aid in the determination of the space these molecules occupy on the surface. Each Br atom is represented by a yellow sphere; oxygens are displayed in red. The parallelograms outline two molecules hydrogen-bonded together, covering three rows of the graphite lattice structure. This conformation is reminiscent of Figure 8a.

The atomically resolved STM topograph of the enantiomorphic *R* domain of 2-bromohexadecanoic acid im-

aged at the liquid—solid interface is displayed in Figure 3a.[49] Again, the COOH groups appear as "dark" topographic depressions, while the Br markers on the same chiral carbon appear as "bright" yellow protrusions. Moreover, those hydrogen atoms on each methylene group that protrude out of the plane of the self-assembly define the hydrocarbon backbone (OC), enclosed by the parallelogram. The direction of the hydroxyl group (OD) corresponds to the edge of the dark COOH spot. Here, the molecular axis-to-hydroxyl group angle (COD), β, becomes $53 \pm 5°$. Molecular models for (*R*)-2-bromohexadecanoic acid are pictured in Figure 3c. Once again, two parallelograms denote the hydrogen-bonded dimer adopting an all-trans configuration on the surface. Now, however, the molecules occupy four rows on the basal plane of graphite, similar to the structure of Figure 8b.

Adopting the alternate carboxylic acid conformation yields energetically unfavorable configurations for 12-bromododecanoic and 2-bromohexadecanoic acids on the graphite surface. For example, if the carboxyl groups for 12-bromododecanoic acid in Figure 7a and c were to arrange in the pattern from Figure 8b, involving rotation by 180° about the carboxyl carbon—α-carbon bond, the acid molecule dimers would occupy an extra row of graphite, which would lead to energetically unfavorable free space in the assembly and an unstable structure.[54] Likewise, if the COOH functionalities of 2-bromohexadecanoic acid, shown in Figure 3a and c, were to assume the configuration depicted in Figure 8a, vacancies would appear at the interface due to the predisposition of the molecules to maintain both hydrogen-bonding and Br—Br intermolecular interactions, as discussed in the preceding section. Thus, the same functional group (COOH) adopts distinctly different yet energetically similar conformations in different molecules in order to maximize molecule-molecule and molecule—surface interactions.

The electronic and/or physical properties of the substrate may also induce perturbations in self-assembly that can be ascertained using chemical marker groups. For instance, as noted earlier, monolayers of 12-bromododecanoic acid order such that the hydrogen-bonded dimer pairs of molecules (Figure 7a) exhibit different periodic structures on a graphite substrate.[51,56] When these same molecules are imaged on a different surface, MoS$_2$, a new pattern of self-organization arises.[56] This pattern likely results from the change in both physical and electronic properties of the new surface. Physically, MoS$_2$ possesses a larger lattice constant than graphite (3.16 versus 2.46 Å).[57-59] Further, MoS$_2$ is a semiconductor whose surface structure is primarily comprised of Mo d$_{z^2}$ and S p$_z$ orbitals.[58,59] (In contrast, graphite has C p$_z$ orbitals protruding out of the plane of the surface.) Combined, these effects have been reported to lead to interesting changes in monolayer order.[56,60]

As shown elsewhere,[56] two differences between the self-assembled monolayers of 12-bromododecanoic acid on graphite and MoS$_2$ are evident. First, the brominated carboxylic acid molecules are less well resolved on MoS$_2$ than on graphite, an indication of weaker adsorbate—
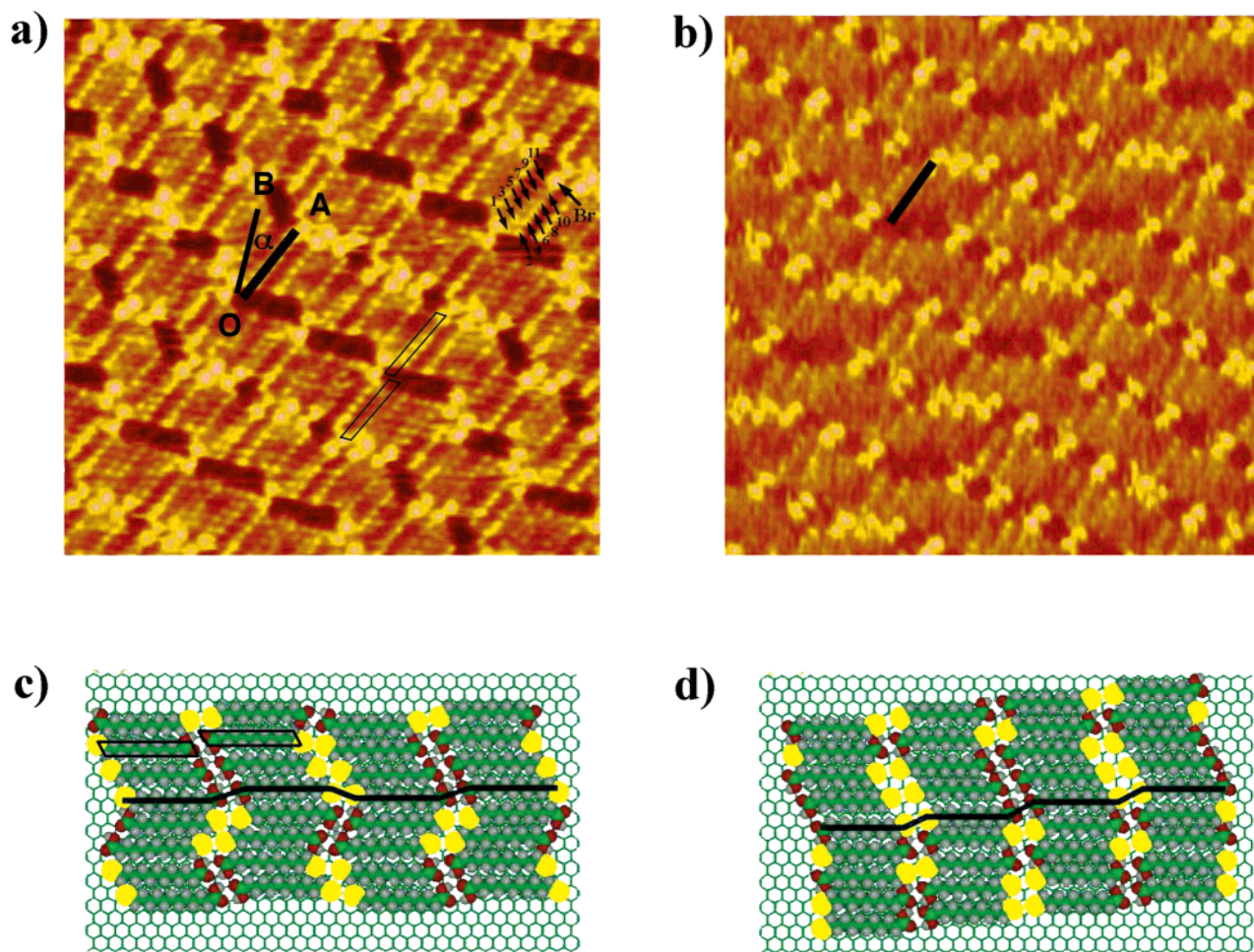
FIGURE 7. (a) 12×12 nm^2 constant current STM image of 12-bromododecanoic acid imaged at the phenyloctane−graphite interface. The "bright" yellow spots (indicative of topographic protrusions) are attributed to the locations of the Br atom end groups. The "dark" topographic depressions are assigned as the positions of the hydrogen-bonding carboxylic acid groups. One molecular length is demarcated by the black bar (OA). In addition to these two marker groups in the image, one hydrogen of each methylene carbon along the molecular backbone is shown, numbered 1−11. The parallelograms outline two acid molecules hydrogen bonded to form a "dimer" pair on the surface. The angle, α, formed by the segment OA and OB, the direction of the hydroxyl group of the acid functionality, is $25 \pm 1°$. (b) 12×12 nm^2 constant current image of 11-bromoundecanoic acid self-assembled on graphite. As in (a), the Br atoms appear as "bright" topographic protrusions; the carboxylic acid groups look like "dark" topographic depressions. The black bar represents one molecular length. (a) and (b) have been obtained at 1.4 V (sample negative) and 300 pA. (c) A molecular model depicting the organization of 12-bromododecanoic acid on a graphite lattice based on the STM image of (a). The model is colored to have the same meaning as Figure 3c. The molecules are organized in an "up"−"down"−"up" progression marked by the black lines. The parallelograms demonstrate that dimers of 12-bromododecanoic acid occupy three rows of the graphite surface. (d) Molecular model of a self-assembled monolayer of 11-bromoundecanoic acid on graphite. Here, the adsorbate−adsorbate interactions effect an upward "stairlike" profile denoted by the black lines.

substrate interactions. Second, monolayer ordering is increased on the semiconductor substrate. Instead of finding periodic dimer structures arranged with a maximum of three pairs together, up to six pairs now define a small domain in the direction orthogonal to the molecular axis. This increase in local order again points to changes in the roles of adsorbate−adsorbate versus adsorbate−substrate interactions. Here, the interaction with the substrate has become weaker, permitting the hydrogen-bonding and Br − Br interactions to dominate.

IV. Summary

When used in conjunction with single and double chemical marker groups that serve as "flags" to elucidate the structural features of an interface, STM provides remark-ably detailed information that can be employed to analyze and ultimately tailor interfacial properties. The absolute chirality of optically active molecules self-assembling on a graphite surface has been determined using these methods. Subtle changes in the orientation of chemical functional groups have been observed and shown to influence the long-range order of the interfacial films. In addition, small changes in the chemical structure of specific molecules have been found to alter self-assembly on graphite surfaces significantly. Variations in the pattern of molecular interfacial ordering for the same film on different surfaces can be easily distinguished using STM. The potential for control of self-assembled structures on surfaces, using a combination of STM tip-induced changes and functional group substitutions, certainly exists and
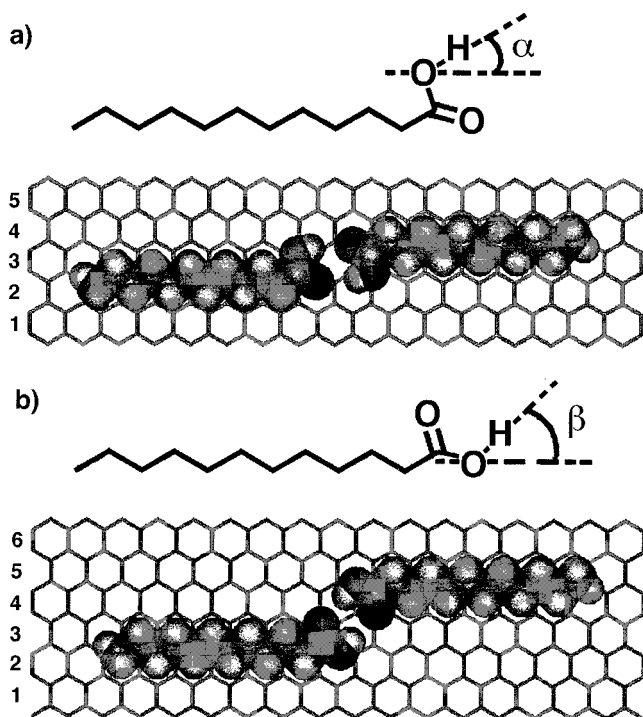
a)

b)

FIGURE 8. (a) Schematic and space-filling representations of dodecanoic acid. The angle between the alkyl chain and the hydroxyl group, α, equals 25°. Two molecules adsorbing on graphite occupy three rows of the lattice, numbered 2−4. (b) Representations of the same dodecanoic acid molecules whose carboxyl groups have been rotated 180° about the carboxyl carbon−α-carbon bond. This yields an angle, β, of 46°. When two molecules with this conformation physisorb on graphite, four rows of the surface (2−5) are covered.

can be followed using the visualization techniques described here.[18−21] STM methods, especially when enhanced by the presence of chemical marker groups, have enormous potential to affect future developments in interfacial science by revealing the structure of monolayer molecular films with unique and important physical and chemical properties.

References

(1) Binnig, G.; Rohrer, H. Scanning Tunneling Microscopy. *Helv. Phys. Acta* **1982**, *55*, 726−735.

(2) Albrecht, T. R.; Quate, C. F. Atomic Resolution with the Atomic Force Microscope on Conductors and Nonconductors. *J. Vac. Sci. Technol. A* **1988**, *6*, 271−274.

(3) Binnig, G.; Quate, C. F.; Gerber, C. Atomic Force Microscope. *Phys. Rev. Lett.* **1986**, *56*, 930−933.

(4) Sarid, D.; Elings, V. Review of Scanning Force Microscopy. *J. Vac. Sci. Technol. B* **1991**, *9*, 431−437.

(5) Frisbie, C. D.; Rozsnyal, L. F.; Noy, A.; Wrighton, M. S.; Lieber, C. M. Functional Group Imaging by Chemical Force Microscopy. *Science* **1994**, *265*, 2071−2074.

(6) Hartmann, U. Magnetic Force Microscopy—Some Remarks from the Micromagnetic Point of View. *J. Appl. Phys.* **1988**, *64*, 1561−1564.

(7) Martin, Y.; Williams, C. C.; Wickramasinghe, H. K. Atomic Force Microscope—Force Mapping and Profiling on a sub 100 Å Scale. *J. Appl. Phys.* **1987**, *61*, 4723−4729.

(8) Binnig, G.; Rohrer, H.; Gerber, C.; Weibel, E. Surface Studies by Scanning Tunneling Microscopy. *Phys. Rev. Lett.* **1982**, *49*, 57−61.

(9) Rohrer, H. Scanning Tunneling Microscopy. *Proc. Natl. Acad. Sci. U.S.A.* **1987**, *84*, 4666.

(10) Binnig, G.; Rohrer, H. Scanning Tunneling Microscopy. *Surf. Sci.* **1985**, *152/153*, 17−26.

(11) Durig, U.; Zuger, P.; Michel, B.; Haussling, L.; Ringsdorf, H. Electronic and Mechanical Characterization of Self-Assembled Alkanethiol Monolayers by Scanning Tunneling Microscopy Combined with Interaction-Force-Gradient Sensing. *Phys. Rev. B* **1993**, *48*, 1711−1717.

(12) Poirier, G.; Pylant, E. The Self-Assembly Mechanism of Alkanethiols on Au(111). *Science* **1996**, *272*, 1145−1148.

(13) Kim, Y.-T.; McCarley, R.; Bard, A. Scanning Tunneling Microscopy Studies of Au(111) Derivatized with Organothiols. *J. Phys. Chem.* **1992**, *96*, 7416−7421.

(14) Hamers, R.; Hovis, J.; Lee, S.; Liu, H.; Shan, J. Formation of Ordered, Anisotropic Organic Monolayers on the Si(001) Surface. *J. Phys. Chem. B* **1997**, *101*, 1489−1492.

(15) Hovis, J.; Lee, S.; Liu, H.; Hamers, R. Controlled Formation of Organic Layers on Semiconductor Surfaces. *J. Vac. Sci. Technol. B* **1997**, *15*, 1153−1158.

(16) Ge, M.; Klemperer, W.; Gewirth, A. Self-Assembly of Silicotungstate Anions on Silver Surfaces. *J. Am. Chem. Soc.* **1996**, *118*, 5812−5813.

(17) Yeo, Y. H.; McGonigal, G. C.; Thomson, D. J. Structural Phase Transition of a 1-Dodecanol Monolayer Physisorbed at the Liquid/Graphite Interface by Scanning Tunneling Microscopy. *Langmuir* **1993**, *9*, 649−651.

(18) Takami, T.; Ozaki, H.; Kasuga, M.; Tsushiya, T.; Mazaki, T.; Fukushi, D.; Ogawa, J.; Uda, M.; Aono, M. Periodic Structure of a Single Sheet of a Clothlike Macromolecule (Atomic Cloth) Studied by Scanning Tunneling Microscopy. *Angew. Chem., Int. Ed. Engl.* **1997**, *36*, 2755−2757.

(19) Grim, P. C. M.; DeFeyter, S.; Gesquiere, A.; Vanoppen, P.; Rucker, M.; Valiyaveetil, S.; Moessner, G.; Mullen, K.; DeSchryver, F. C. Submolecularly Resolved Polymerization of Diacetylene Molecules on the Graphite Surface Observed with Scanning Tunneling Microscopy. *Angew. Chem., Int. Ed. Engl.* **1997**, *36*, 2601−2603.

(20) Nakajima, K.; Ikehara, T.; Nishi, T.; Hashizume, T.; Heike, S.; Watanabe, S.; Wada, Y. Direct Observation of Topochemical-photopolymerizable Single Organic Molecule Adsorbed on Si-(100) by STM. *J. Kor. Phys. Soc.* **1997**, *31*, S39−S43.

(21) Yablon, D. G.; Giancarlo, L. C.; Flynn, G. W. Manipulating Self-Assembly with Achiral Molecules: An STM Study of Chiral Segregation by Achiral Adsorbates. *J. Phys. Chem. B*, submitted.

(22) Hibino, M. S., A.; Tsuchiya, H.; Hatta, I. Microscopic Origin of the Odd−Even Effect in Monolayer of Fatty Acids Formed on a Graphite Surface by Scanning Tunneling Microscopy. *J. Phys. Chem. B* **1998**, *102*, 4544−4547.

(23) Venkataraman, B.; Flynn, G. W.; Wilbur, J.; Folkers, J. P.; Whitesides, G. M. Differentiating Functional Groups with the Scanning Tunneling Microscope. *J. Phys. Chem.* **1995**, *99*, 8684−8689.

(24) Cyr, D. M.; Venkataraman, B.; Flynn, G. W.; Black, A.; Whitesides, G. M. Functional Group Identification in Scanning Tunneling Microscopy of Molecular Adsorbates. *J. Phys. Chem.* **1996**, *100*, 13747−13759.

(25) Cyr, D. M.; Venkataraman, B.; Flynn, G. W. STM Investigations of Organic Molecules Physisorbed at the Liquid−Solid Interface. *Chem. Mater.* **1996**, *8*, 1600−1615.

(26) Sheng, H. Y.; Dong, Z. C.; Fujita, D.; Ohgi, T.; Jiang, Q. D.; Nejoh, H. Two-dimensional Ordering of Octadecanethiol Molecules on Graphite Observed by Scanning Tunneling Microscope. *Appl. Surf. Sci.* **1997**, *121/122*, 129−132.

(27) Stipe, B. C.; Rezaei, M. A.; Ho, W. Single-molecule Vibrational Spectroscopy and Microscopy. *Science* **1998**, *280*, 1732−1735.

(28) Gaudioso, J.; Lee H. J.; Ho, W. Vibrational Analysis of Single Molecule Chemistry: Ethylene Dehydrogenation on Ni(110). *J. Am. Chem. Soc.* **1999**, *121*, 8479−8485.

(29) Wolkow, R. A. Controlled Molecular Adsorption on Silicon: Laying a Foundation for Molecular Devices. *Annu. Rev. Phys. Chem.* **1999**, *50*, 413−441.

(30) Shan, J.; Wang, Y. J.; Hamers, R. J. Adsorption and Dissociation of Phosphine on Si(001). *J. Phys. Chem.* **1996**, *100*, 4961−4969.

(31) Foley, E. T.; Kam, A. F.; Lyding, J. W.; Avouris, P. Cryogenic UHV−STM Study of Hydrogen and Deuterium Desorption from Si(100). *Phys. Rev. Lett.* **1998**, *80*, 1336−1339.

(32) Martel, R.; Avouris, P.; Lyo, I. W. Molecularly Adsorbed Oxygen Species on Si(111)−(7 × 7): STM-induced Dissociative Attachment Studies. *Science* **1996**, *272*, 385−388.

(33) Weiss, P. S.; Eigler, D. M. Site Dependence of the Apparent Shape of a Molecule in Scanning Tunneling Microscope Images—Benzene on Pt(111). *Phys. Rev. Lett.* **1993**, *71*, 3139−3142.

(34) Lu, X.; Hipps, K. W. Scanning Tunneling Microscopy of Metal Phthalocyanines: d(6) and d(8) Cases. *J. Phys. Chem. B* **1997**, *101*, 5391−5396.

(35) Tao, N. J. Probing Potential-tuned Resonant Tunneling Through Redox Molecules with Scanning Tunneling Microscopy. *Phys. Rev. Lett.* **1996**, *76*, 4066−4069.

(36) Claypool, C. L.; Faglioni, F.; Goddard, W. A.; Gray, H. B.; Lewis, N. S.; Marcus, R. A. Source of Image Contrast in STM Images of Functionalized Alkanes on Graphite: A Systematic Functional Group Approach. *J. Phys. Chem. B* **1997**, *101*, 5978−5995.

(37) Ikai, A. STM and AFM of Bio/Organic Molecules and Structures. *Surf. Sci. Rep.* **1996**, *26*, 261−332.

(38) Takeuchi, H.; Kawauchi, S.; Ikai, A. Differentiation of Chemically Functional Groups in Stearoyl Amide and Anilide with Scanning Tunneling Microscopy. *Jpn. J. Appl. Phys.* **1996**, *35*, 3754−3758.

(39) Yoshimura, K.; Arakawa, H.; Ikai, A. Scanning Tunneling Imaging of Bio-Organic Molecules and Their Tunneling Properties: Fatty Acids, Their Derivatives and Cholesteryl Stearate. *Jpn. J. Appl. Phys.* **1995**, *34*, 3368−3372.

(40) Giancarlo, L. C.; Flynn, G. W. Scanning Tunneling and Atomic Force Microscopy Probes of Self-Assembled, Physisorbed Monolayers: Peeking at the Peaks. *Annu. Rev. Phys. Chem.* **1998**, *49*, 297−336.

(41) Lazzaroni, R.; Calderone, A.; Bredas, J. L.; Rabe, J. P. Electronic Structure of Molecular van der Waals Complexes with Benzene: Implications for the Contrast in Scanning Tunneling Microscopy of Molecular Adsorbates on Graphite. *J. Chem. Phys.* **1997**, *107*, 99−105.

(42) *Handbook of Chemistry and Physics*, 71st ed.; CRC Press: Boston, 1990−91.

(43) Hibino, M.; Sumi, A.; Hatta, I. Molecular Arrangements of Fatty Acids and Cholesterol at Liquid/Graphite Interface Observed by Scanning Tunneling Microscopy. *Jpn. J. Appl. Phys.* **1995**, *34*, 3354−3359.

(44) Hibino, M.; Sumi, A.; Hatta, I. Atomic Images of Saturated and Unsaturated Fatty Acids at Liquid/Graphite Interface and Difference of Tunneling Currents between Them Observed by Scanning Tunneling Microscopy. *Jpn. J. Appl. Phys.* **1995**, *34*, 610−614.

(45) Stabel, A.; Dasaradhi, L.; O'Hagan, D.; Rabe, J. P. Scanning Tunneling Microscopy Imaging of Single Fluorine Atom Substitution in Stearic Acid. *Langmuir* **1995**, *11*, 1427−1430.

(46) Hatta, I.; Nichino, J.; Sumi, A.; Hibino, M. Ordered Structure Formed by Biologically Related Molecules. *Jpn. J. Phys.* **1995**, *34*, 3930−3936.

(47) Crystal, J. B.; Zhang, L. Y.; Friesner, R. A.; Flynn, G. Computational Modeling for Scanning Tunneling Microscopy of Physisorbed Molecules via Ab Initio Quantum Chemistry, submitted.

(48) Palmer, A. G., III; Williams, J.; McDermott, A. Nuclear Magnetic Resonance Studies of Biopolymer Dynamics. *J. Phys. Chem.* **1996**, *100*, 13293−13310.

(49) Fang, H.; Giancarlo, L. C.; Flynn, G. W. Direct Determination of the Chirality of Organic Molecules by Scanning Tunneling Microscopy. *J. Phys. Chem. B* **1998**, *102*, 7311−7315.

(50) X-ray crystallography of purified (R)/(S)-2-bromohexadecanoic acid revealed crystals composed of both enantiomers bonded together. Parkin, G., personal communication.

(51) Fang, H.; Giancarlo, L. C.; Flynn, G. W. Packing of $Br(CH_2)_{10}COOH$ and $Br(CH_2)_{11}COOH$ on Graphite: An Odd−Even Length Effect Observed by Scanning Tunneling Microscopy. *J. Phys. Chem. B* **1998**, *102*, 7421−7424.

(52) Venkataraman, B.; Breen, J. J.; Flynn, G. W. Scanning Tunneling Microscopy Studies of Solvent Effects on the Adsorption and Mobility of Triacontane/Triacontanol Molecules Adsorbed on Graphite. *J. Phys. Chem.* **1995**, *99*, 6608−6619.

(53) Rabe, J. P.; Buchholz, S. Commensurability and Mobility in Two-dimensional Molecular Patterns on Graphite. *Science* **1991**, *253*, 424−427.

(54) Fang, H.; Giancarlo, L. C.; Flynn, G. W. Identification of the Conformation of Individual Molecules by Scanning Tunneling Microscopy. *J. Phys. Chem. B* **1999**, *103*, 5712−5715.

(55) Based on calculations performed using Spartan program for *n*-hexadecanoic and 2-bromohexadecanoic acids.

(56) Giancarlo, L. C.; Fang, H.; Rubin, S. M.; Bront, A. A.; Flynn, G. W. Influence of the Substrate on Order and Image Contrast for Physisorbed, Self-Assembled Molecular Monolayers: STM Studies of Functionalized Hydrocarbons on Graphite and MoS_2. *J. Phys. Chem. B* **1998**, *102*, 10255−10263.

(57) Pisanty, A. The Electronic Structure of Graphite: A Chemist's Introduction to Band Theory. *J. Chem. Educ.* **1991**, *68*, 804−808.

(58) Coley, T. R.; Goddard, W. A.; Baldeschwieler, J. D. Theoretical Interpretation of Scanning Tunneling Microscopy Images: Application to the Molybdenum Disulfide Family of Transition Metal Dichalcogenides. *J. Vac. Sci. Technol.* **1991**, *9*, 470−474.

(59) Henson, T. D.; Sarid, D.; Bell, S. STM of Layered-structure Semiconductors. *J. Microsc.* **1988**, *152*, 467−472.

(60) Cincotti, S.; Rabe, J. P. Self-assembled Alkane Monolayers on $MoSe_2$ and MoS_2. *Appl. Phys. Lett.* **1993**, *62*, 3531−3533.

AR970261M